

High Affinity Chimeric Antigen Receptor with Cross-Reactive scFv to Clinically Relevant EGFR Oncogenic Isoforms

1 **Radhika Thokala**^{1,2,□}, **Zev A. Binder**^{1,2,□}, **Logan Zhang**^{1,2}, **Jiasi Vicky Zhang**^{1,2}, **Daniel Y.**
2 **Zhang**^{2,3}, **Michael C. Milone**^{2,4}, **Guo-li Ming**³, **Hongjun Song**^{2,5}, **Donald M. O'Rourke**^{1,2,*}

3 ¹Laboratory X, Institute X, Department X, Organization X, City X, State XX (only USA, Canada and
4 Australia), Country

5 ¹Department of Neurosurgery, Perelman School of Medicine, University of Pennsylvania,
6 Philadelphia, PA, USA.

7 ²GBM Translational Center of Excellence, Abramson Cancer Center, Perelman School of Medicine,
8 University of Pennsylvania, Philadelphia, PA, USA

9 ³Biochemistry and Molecular Physics Graduate Group, Perelman School of Medicine, University of
10 Pennsylvania, Philadelphia, PA, USA

11 ⁴Department of Pathology and Laboratory Medicine, Perelman School of Medicine, University of
12 Pennsylvania, Philadelphia, PA, USA

13 ⁵Department of Neuroscience and Mahoney Institute for Neurosciences, Perelman School of
14 Medicine, University of Pennsylvania, Philadelphia, PA, USA

15 □These authors have contributed equally to this work and share first authorship

16
17 ***Correspondence:**

18 Donald M. O'Rourke, M.D
19 John Templeton, Jr. M.D Professor in Neurosurgery
20 Director, Glioblastoma Translational Center of Excellence (TCE)
21 The Abramson Cancer Center
22 Perelman School of Medicine
23 The University of Pennsylvania
24 Philadelphia, PA 19104
25 Telephone: 215-662-3490
26 donald.orourke@pennmedicine.upenn.edu

27 **Keywords: GBM, Glioma, Immunotherapy, CAR T Cells, Adoptive T Cell Therapy, EGFR.**

28

29 **Abstract**

30 Tumor heterogeneity is a key reason for therapeutic failure and tumor recurrence in glioblastoma
31 (GBM). Our chimeric antigen receptor (CAR) T cell (2173 CAR T cells) clinical trial
32 (NCT02209376) against Epidermal growth factor receptor (EGFR) variant III (EGFRvIII)
33 demonstrated successful trafficking of T cells across the blood brain barrier into GBM active tumor

806-CAR in Glioblastoma

34 sites. However, CAR T cell infiltration was associated only with a selective loss of EGFRvIII⁺
35 tumor, demonstrating little to no effect on EGFRvIII⁻ tumor cells. Post-CAR T treated tumor
36 specimens showed continued presence of EGFR amplification and oncogenic EGFR extracellular
37 domain (ECD) missense mutations, despite loss of EGFRvIII. To address tumor escape, we generated
38 an EGFR-specific CAR by fusing monoclonal antibody (mAb) 806 to a 4-1BB co-stimulatory
39 domain. The resulting construct was compared to 2173 CAR T cells in GBM, using in vitro and in
40 vivo models. 806 CAR T cells specifically lysed tumor cells and secreted cytokines in response to
41 amplified EGFR, EGFRvIII, and EGFR-ECD mutations in U87MG cells, GBM neurosphere-derived
42 cell lines, and patient-derived GBM organoids. 806 CAR T cells did not lyse fetal brain astrocytes or
43 primary keratinocytes to a significant degree. They also exhibited superior antitumor activity in vivo
44 when compared to 2173 CAR T cells. The broad specificity of 806 CAR T cells to EGFR alterations
45 gives us the potential to target multiple clones within a tumor and reduce opportunities for tumor
46 escape via antigen loss.

47

48 Introduction

49 Chimeric antigen receptor (CAR) cells targeting pediatric B cell malignancies have shown
50 unprecedented responses and were the first CAR T cell therapies to receive FDA approval, in 2017
51 (1-3). The successful application of this therapeutic technology in the treatment of solid tumors,
52 including glioblastoma (GBM), remains a significant challenge; chief among them are tumor
53 heterogeneity, immunosuppressive tumor microenvironment, and antigen escape (4, 5). Successful
54 strategies for overcoming these obstacles are required to advance CAR T therapy in solid tumors.

55

56 Epidermal growth factor receptor (EGFR) was one of the first oncogenes identified in GBM and
57 presents an attractive therapeutic target, given its extracellular nature and frequent alterations in
58 GBM. Approximately 60% of GBM specimens contain a mutation, rearrangement, splicing
59 alteration, and/or amplification of EGFR (6). EGFR overexpression, mediated through focal
60 amplification of the EGFR locus as double minute chromosomes, has long been recognized as the
61 most common EGFR alteration, present in 60% of GBM patients (7, 8). Tumor-specific EGFR
62 variant III (EGFRvIII), resulting from deletion of exon 2-7 of wildtype EGFR (wtEGFR), is present
63 in 30% of GBM patients (9). In addition, oncogenic missense mutations EGFR^{A289D/T/V}, EGFR^{R108G/K},
64 and EGFR^{G598V} have been identified in 12-13% of cases in the extracellular domain (ECD) of EGFR,
65 independent of EGFRvIII. Missense mutations and EGFRvIII often co-occur with EGFR
66 amplification and activate EGFR receptor independent of its ligand (10). Several of the missense
67 mutations have been shown to have a negative effect on patient survival, driving tumor proliferation
68 and invasion (11).

69

70 Our first-in-man CAR T clinical trial (NCT02209376) against EGFRvIII in recurrent GBM
71 demonstrated the safety of a peripheral infusion of CAR T cells and resulted in successful trafficking
72 of the CAR T cells to active tumor sites, across the blood brain barrier (12). After treatment, CAR T
73 cells infiltrated the GBM tumors rapidly, proliferated in situ, and persisted over a prolonged period of
74 time. However, CAR T cell infiltration was associated only with a selective loss of EGFRvIII⁺ GBM
75 cells. Importantly, post-CAR T treated tumor specimens showed the continued presence of EGFR
76 amplification and missense mutations, despite the decrease in EGFRvIII target antigen. Persistence of

77 EGFR amplification and ECD missense mutations in the context of loss of EGFRvIII expression
78 suggested tumor heterogeneity played an essential role for tumor recurrence and continued regrowth.

79

80 mAb806, originally raised against EGFRvIII, recognizes a conformationally exposed epitope of
81 wtEGFR when it is overexpressed on tumor cells. The same epitope is not exposed in EGFR
82 expressed on normal non-overexpressing cells (13, 14). ABT-414, an antibody-drug conjugate
83 composed of a humanized mAb806 (ABT-806), showed early efficacy in phase I/II clinical trials
84 with no apparent skin toxicity in treated GBM patients (15). However, a recent Phase III trial was
85 terminated when an interim analysis failed to demonstrate a survival benefit over placebo (16).
86 mAb806 showed an increased binding affinity for not only EGFRvIII but also EGFR ECD mutations
87 and a low affinity for wtEGFR (11). These findings suggest that mAb806 is a viable therapeutic
88 option for tumors harboring EGFR alterations in addition to EGFRvIII.

89 In the present study, we have developed EGFR-specific CAR T cells derived from the single chain
90 fragment variable region (scFv) of 806 mAb, using our standard 4-1BB- ζ construct (17). We then
91 compared 806 CAR T activity with EGFRvIII-specific CAR T cells (2173 CAR T), currently in
92 clinic, for specificity against oncogenic EGFR alterations, including amplified EGFR, EGFRvIII, and
93 extracellular mutations *in vitro* and *in vivo*.

94

95 **Materials and Methods**

96 **CAR constructs**

97 806 scFvs were swapped with scFv of our standard CD19-BB- ζ lentiviral vector described previously
98 to generate 806-BB- ζ CAR (17, 18). Briefly, the nucleotide coding sequences of 806 or C225 scFv
99 with huCD8 leader were synthesized by Geneart (Thermo Fisher Scientific, Waltham, MA) with 5'
100 XbaI and 3'NheI and ligated to XbaI and NheI sites of CD19-BB- ζ car construct. The C225-BB- ζ
101 CAR was obtained from Dr. Avery Posey's lab at the University of Pennsylvania. The 2173-BB- ζ
102 CAR T construct was obtained from Dr. Laura Johnson's Lab at the University of Pennsylvania (19,
103 20).

104

105 **Transduction and expansion of primary human T lymphocytes**

106 Human primary total T cells (CD4 and CD8) were isolated from normal healthy donors following
107 leukapheresis by negative selection using RosetteSep kits (Stemcell Technologies, Vancouver, CA).
108 All specimens were collected with protocol approved by University Review Board and written
109 informed consent was obtained from each donor. T cells were cultured in RPMI 1640 (Thermo Fisher
110 Scientific) supplemented with 10% fetal bovine serum (FBS) (VWR, Radnor, PA), 10 mM HEPES
111 (Thermo Fisher Scientific), 100 U/mL penicillin (Thermo Fisher Scientific), 100 g/mL streptomycin
112 sulfate (Thermo Fisher Scientific), and stimulated with magnetic beads coated with anti-CD3/anti-
113 CD28 (Thermo Fisher Scientific) at 1:3 T cell to bead ratio. Approximately 24 hours after activation,
114 T cells were transduced with lentiviral vectors encoding CAR transgene at an MOI of 3 to 6. On day
115 5 beads were removed and thereafter cells were counted and fed every 2 days, supplemented with IL
116 2 150 U/mL until they were either used for functional assays or cryopreserved for future use.

117

118 **Cell lines and cell culture**

806-CAR in Glioblastoma

119 The human cell line U87MG was purchased from the American Type Culture Collection (ATCC)
120 and maintained in MEM (Richter's modification) (Thermo Fisher Scientific) with components
121 GlutaMAX-1 (Thermo Fisher Scientific), HEPES pyruvate, and penicillin/streptomycin
122 supplemented with 10% FBS. Primary human keratinocytes were purchased from the Dermatology
123 Core Facility at the University of Pennsylvania. K562 cells were purchased from ATCC and
124 maintained in RPMI media (Invitrogen, Carlsbad, CA) supplemented with 10% FBS, 20 mM
125 HEPES, and 1% penicillin/streptomycin. Primary astrocytes were purchased (Sciencell Research
126 Laboratories, Carlsbad, CA) and cultured according to manufacture instructions. The cells from early
127 passages were used for cytotoxicity and cytokine experiments. GSC cell lines were cultured in
128 DMEM F12 media (Sigma Aldrich, St. Louis, MO) supplemented with 2% B27 without vitamin A
129 (Thermo Fisher Scientific), 20 mM HEPES, and penicillin/streptomycin.

130

131 **EGFR-mutant cell lines**

132 To produce the overexpressing EGFR cell line (designated as U87MG-EGFR), lentivirus co-
133 expressing wtEGFR and Cyan Fluorescent Protein (CFP) under the control of EF-1 α promoter was
134 transduced into U87MG cell line. On post-transduction day 4, cells were sorted on an Influx cell
135 sorter (BD, Franklin Lakes, NJ) on the basis of high EGFR expression, and subsequently expanded.
136 Lentivirus co-expressing CFP and EGFR mutants EGFR^{R108K/G}, EGFR^{A289D/T/V}, or EGFRvIII were
137 transduced into U87MG-EGFR, GSC5077 neurosphere cells (21), and K562 cell lines. CFP positive
138 cells were sorted by fluorescence activated cell sorting (FACS). For luciferase killing assays and in
139 vivo tracking studies, U87MG and U87MG-EGFR mutant cell lines were transduced with lentivirus
140 click beetle green (CBG) luciferase and Green Fluorescent protein (GFP). Anti-GFP positive cells
141 were sorted by FACS.

142

143 **Cytokine analysis**

144 CAR T cells and K562 targets expressing EGFR and its variants were co-cultured in 1:2 ratio in R10
145 medium in a 96 well plate, in triplicate. Plates were incubated at 37°C with 5% CO₂. After 48 hours,
146 supernatants were collected and cytokine levels were assessed by ELISA kit (R&D Systems,
147 Minneapolis, MN) for IFN- γ , TNF- α , and IL2 production, according to manufacture instructions.

148

149 **Chromium release assay**

150 The cytolytic efficacy of CAR T cells against K562 cells was evaluated by 4-hour chromium release
151 assays using E:T ratios of 5:1, 2.5:1, and 1:1. ⁵¹Cr labeled target cells were incubated with CAR T
152 cells in complete medium or 0.1% Triton X-100, to determine spontaneous and maximum ⁵¹Cr
153 release respectively, in a V-bottomed 96-well plate. The mean percentage of specific cytolysis of
154 triplicate wells was calculated from the release of ⁵¹Cr using a Top Count NXT (Perkin-Elmer Life
155 and Analytical Sciences, Inc., Waltham, MA) as:

$$156 \quad 100 \times \frac{(\text{experimental release} - \text{spontaneous release})}{(\text{maximal release} - \text{spontaneous release})}$$

157 Data was reported as mean \pm SD.

158

159 **Luciferase based Cytotoxic Assay**

160 CBG+ target cell lines (U87 variants and GSC5077 variants) were co-cultured with CAR T cells at
161 E:T ratios of 10:1, 5:1, and 2.5:1, for 24 hours at 37°C. 100 µL of the mixture was transferred to a 96
162 well black luminometer plate, 100µL of 66 µg/mL D-luciferin (Goldbio, St. Louis, MO) was added,
163 and the luminescence was immediately determined. Results were reported as percent killing based on
164 luciferase activity in wells with tumor cells alone.

165

166 **CD107a degranulation**

167 To assess CD107a degranulation, we plated 1×10^5 T cells and 5×10^5 stimulator target cells per well
168 in round-bottom 96-well plates, to a final volume of 200 µL in complete R10 medium, in triplicates.
169 CD107a-PE antibody (BD) was added into each well and incubated at 37°C for 4 hours, along with
170 surface staining for CD8 (Biolegend, San Diego, CA) and CD3 and then analyzed by flow cytometry.

171

172 **Flow cytometry**

173 For CAR detection, cells were stained with biotinylated protein L (GenScript, Piscataway, NJ), goat
174 anti-mouse IgG, and anti-human IgG (Jackson ImmunoResearch Laboratories, West Grove, PA),
175 followed by streptavidin-conjugated Allophycocyanin (APC) (BD). Surface expression of EGFR and
176 its mutants was detected by CFP and APC-conjugated cetuximab antibody (Novus Biologicals,
177 Centennial, CO). EGFRvIII expression was detected by anti-EGFRvIII Antibody, clone DH8.3
178 (Santa Cruz Biotechnology, Dallas, TX). Flow analysis done by LSR Fortessa (BD) and data were
179 analyzed by FlowJo software (BD).

180

181 **Animal experiments**

182 All mouse experiments were conducted according to Institutional Animal Care and Use Committee
183 (IACUC)–approved protocols. NSG mice were injected with 2.5×10^5 U87MG-
184 EGFR/EGFRvIII/Luc+ tumors subcutaneously in 100 µL of PBS on day 0, 7 animals per cohort.
185 Tumor progression was evaluated by luminescence emission on a IVIS Lumin III In Vivo Imaging
186 System (Caliper Life Sciences, Hopkinton, MA) after intraperitoneal D-luciferin injection according
187 to the manufacturer’s instructions (GoldBio). Tumor size was measured by calipers in two
188 dimensions and approximated to volume using the following calculation:

$$Volume = \frac{L \times \pi W^2}{6}$$

189 Seven days after tumor implantation, mice were treated with 3×10^6 CAR T cells intravenously via the
190 tail vein, in 100 µL of PBS. Survival was followed over time until predetermined IACUC-approved
191 endpoints were reached.

192

193 **GBM organoids**

194 GBM organoids (GBOs) were established from primary patient tissue, under a University of
195 Pennsylvania Institutional Review Board approved protocol and with patient written informed
196 consent, and co-cultured with CAR T cells as described previously (22, 23). GBOs were fixed and
197 stained after co-culture, using anti-CD3 (BioLegend), anti-cleaved caspase 3 (Cell Signaling
198 Technology, Danvers, MA), anti-EGFR (Thermo Fisher Scientific), anti-EGFRvIII (Cell Signaling
199 Technology), and DAPI (Sigma). To control for tumor heterogeneity, 4 GBOs per condition were

806-CAR in Glioblastoma

200 used. Mutational data and variant allele fractions (VAF) were obtained from the Center for
201 Personalized Diagnostics at the University of Pennsylvania, as described previously (24).

202

203 **Statistical analysis**

204 All in vitro experiments were performed at least in triplicate. GraphPad Prism 6 software (GraphPad
205 Software, San Diego, CA) was used for statistical analyses. Data were presented as mean \pm standard
206 deviation. The differences between means were tested by appropriate tests. For the mouse
207 experiments, changes in tumor radiance from baseline at each time point were calculated and
208 compared between groups using t-test or Wilcoxon rank-sum test, as appropriate. Survival
209 determined from the time of T cell injection was analyzed by the Kaplan-Meier method and
210 differences in survival between groups were compared by log-rank Mantel-Cox test.

211

212 **Results**

213 **Generation of 806 CARs and Cell lines expressing EGFR mutated proteins**

214 In the present study, we have generated CARs that target EGFR and EGFR mutants by fusing the
215 scFv derived from mAb806 to a 2nd generation CAR construct containing 4-1BB-CD3 ζ signaling 806
216 CAR, the design of which is shown schematically in Fig. 1A. The EGFRvIII-specific 4-1BB-CD3 ζ
217 based 2173 CAR used in our clinical trials (NCT02209376 and NCT03726515) was generated for
218 comparative evaluation with 806 CAR. 4-1BB based Cetuximab (C225) and CD19 CARs were used
219 as positive and negative controls. Lentiviral vectors encoding CARs were transduced into a mixture of
220 CD4 and CD8 T cells and surface expression was confirmed by flow cytometry (Fig. 1B). We next
221 turned to generating target-positive tumor cell lines, expressing the mutations EGFR^{R108K/G},
222 EGFR^{A289D/T/V}, EGFR^{G598V}, and EGFRvIII, for testing of our CAR constructs (Fig. 1C). In order to
223 more faithfully model the EGFR mutations, which are almost always co-expressed with amplified
224 wtEGFR, we transduced the GBM cell line U87MG and patient-derived glioma stem cell line
225 GSC5077 (21), both of which express low levels of wtEGFR, with a lentiviral vector encoding
226 wtEGFR (Fig.1D) (resultant lines referred to as U87MG-EGFR and GSC5077-EGFR), as well as
227 K562 chronic myelogenous leukemia (CML) cells that lack endogenous expression of EGFR, with
228 wtEGFR (Fig. 1E). U87MG-EGFR, GSC5077-EGFR, and K562 cells were also transduced with
229 EGFRvIII lentivirus and expression was then analyzed by an EGFRvIII-specific antibody (Fig.1F). A
230 lentiviral vector co-expressing CFP and the targeted EGFR extracellular mutants (Fig.1D) was
231 transduced into U87MG-EGFR, GSC5077-EGFR, and K562 cells. The resulting CFP positive cells
232 were sorted by fluorescence-activated cell sorting to obtain a positively transduced cell population
233 (Fig. 1G).

234

235 ***In vitro* characterization of 806 CAR T cells**

236 To determine the specificity of the 806 and 2173 CARs for overexpressed wtEGFR, EGFRvIII, and
237 the EGFR-ECD mutants, 2173 and 806 EGFR BB- ζ CAR T cells were co-cultured with U87MG-
238 EGFR and GSC5077-EGFR cell lines expressing EGFRvIII and extracellular mutants EGFR^{R108K/G},
239 EGFR^{A289D/T/V}, and EGFR^{G598V}, in 24-hour bioluminescence-luciferase based killing assays (Fig. 2A-
240 B). While 2173 CAR T cells demonstrated specificity for EGFRvIII alone, 806 CAR T cells efficiently
241 lysed all targets and exhibited similar cytolytic potential as C225 CAR T (Fig. 2A-B). Notably, 806
242 CAR T cells were able to kill U87MG cells, despite expressing only low levels of wtEGFR, at an

243 equal level when compared to overexpressed wtEGFR and EGFRvIII. Since U87MG-EGFR mutants
244 expressed endogenous and ectopic EGFR, we could not distinguish if the 806 scFv binding
245 specificity was restricted to the mutant or wtEGFR. To test the exclusive specificity to the mutants,
246 we co-cultured 806 and 2173 CAR T cells with the CML cell line K562, transduced to express
247 wtEGFR, EGFRvIII, or EGFR-mutants, as K562 does not have any endogenous EGFR (Fig. 2B).
248 806 CAR T cells did not lyse untransduced K562 cells, confirming the lack of EGFR on the parental
249 line. The 806 CAR T cells selectively targeted K562 cells expressing EGFR, EGFRvIII, or EGFR-
250 ECD mutants and demonstrated similar efficacy as C225 CAR T cells. 2173 CAR T cells lysed
251 K562-EGFRvIII cells but did not show any activity against either wtEGFR or the ECD mutants, as
252 expected (Fig. 2B). T cell activation was assessed by induction of surface CD107a expression after
253 co-culture of CAR T cells with target-expressing cells (Fig. 2C). Antigen-specific effector cytokine
254 production was assessed by co-culturing K562 target cells transduced with EGFR and its variants
255 with CAR T cells. The resulting supernatants were analyzed for IFN- γ , TNF- α , and IL2 production
256 (Fig. 2D). Untransduced K562 and Nalm6 cells were used as negative controls. 806 and C225 CAR
257 T cells produced similar levels of CD107 degranulation (Fig. 2C) and IFN- γ , TNF- α , and IL2 (Fig.
258 2D) in response to EGFRvIII, EGFR-ECD mutants, and EGFR overexpressing cells, while 2173
259 CAR T cells responded to EGFRvIII alone.

260

261 **806 CAR T cells exhibit low or no affinity for EGFR expressed on primary astrocytes and** 262 **keratinocytes**

263 Having confirmed the function of the 806 CARs, we next sought to compare the reactivity of 806 and
264 2173 CAR T cells in response to endogenous levels of EGFR in normal cells, *in vitro*. We cultured
265 primary human keratinocytes and astrocytes, as those cell types express wtEGFR (Fig. 3A) and used
266 them to stimulate CAR T cells. We observed production of IFN- γ by C225 CAR T cells, in response
267 to EGFR presented by either astrocytes or keratinocytes, as well as U87MG-EGFR (Fig. 3B). In
268 contrast, 2173 CAR T cells produced IFN- γ in response to EGFRvIII antigen alone. 806 CAR T cells
269 exhibited low or no cytotoxicity when co-cultured with astrocytes or keratinocytes (Fig. 3C), with
270 corresponding low IFN- γ production (Fig. 3B).

271

272 **Anti-tumor activity of 806 CAR T cells in *in vivo***

273 Having compared the antigen specific effector function of 806 CAR with 2173CARs, we next sought
274 to confirm its *in vivo* anti-tumor effects, using immunodeficient NSG mice bearing human GBM
275 tumors (Fig. 4A). On Day 0, U87MG-EGFR/EGFRvIII tumors were implanted subcutaneously and
276 on Day 5, tumor engraftment was confirmed by bioluminescence imaging (BLI). On Day 7, a single
277 dose of 3×10^6 CAR positive T cells were infused intravenously (n = 7 per cohort). Total
278 bioluminescence (Fig. 4B) and individual bioluminescence (Fig. 4C) was assessed in 806 and 2173
279 CAR T cell treated groups. Animals in the negative control cohort, receiving CD19 CAR T cells,
280 demonstrated rapid tumor growth, with all mice reaching a predetermined humane experimental
281 endpoint by 42 days after initial tumor engraftment. To be noted, all mice in the CD19, 2173, and
282 806 groups reached experimental endpoint by day 42, 63, and 91 days, respectively (Fig. 4A).

283

284 **High fidelity GBM organoids demonstrate cross-reactivity of 806 CAR**

285 Given the ability of the 806 CAR to target EGFR alterations beyond EGFRvIII, we turned to patient-
286 derived GBM organoids (GBOs) to demonstrate activity in a heterogenous model previously
287 characterized to be of high fidelity to human tumors (22, 23). GBOs retain the originating tumor

806-CAR in Glioblastoma

288 heterogeneity to a high degree out beyond 12 weeks of culturing and maintain expression of
289 endogenous EGFR and its alterations, providing a valuable model platform for testing therapies
290 aimed at addressing tumor escape. The GBOs selected for co-culture experiments contained multiple
291 EGFR mutations (Fig. 5A). GBO 9057 had EGFR copy number gain, EGFRvIII, and two missense
292 mutations, EGFR^{G598V} and EGFR^{C595Y}. The missense mutation was found to have a VAF of 24%,
293 while EGFRvIII was identified in less than 10% of the reads, based on next generation sequencing
294 (NGS). GBO 9066 had EGFR copy number gain, EGFR^{A289V}, and EGFR^{G598V}. Both EGFR^{A289V} and
295 EGFR^{G598V} had a VAF of less than 15%, making determination of co-occurrence impossible through
296 NGS.

297

298 GBOs were co-cultured with 806, 2173, and CD19 CAR T cells, at a 1:10 E:T ratio, for 72 hours
299 before fixation and evaluation. CAR T cell infiltration, as quantified by CD3 staining, was more
300 significant in the 806 CAR T cell population than either the 2173 or CD19 CAR T cell population
301 (Fig. 5B). Cleaved caspase 3 (CC3) was used as a measure of cell death and anti-tumor activity. As
302 with the CD3⁺ cell infiltration, the 806 CAR co-culture resulted in higher CC3 levels than either the
303 2173 or CD19 CAR co-cultures (Fig. 5C). These results highlighted the broad cross-reactivity of the
304 806 CAR in a heterogeneous, high-fidelity GBM model. wtEGFR staining in both GBO lines
305 provided additional evidence of the cross-reactive nature of the 806 CAR (Fig. 5D). Staining
306 intensity, normalized to CD19 CAR-treated GBOs, showed consistent decreases in 806 CAR-treated
307 GBOs, to a greater degree than the 2173 CAR-treated GBOs (Fig. 5E).

308 Discussion

309 We have shown broad cross-reactivity of 806 CAR T cells to EGFR mutant proteins resulting in
310 enhanced anti-GBM tumor killing, along with a low on-target, off-tumor effect against both
311 astrocytes and keratinocytes that express wildtype EGFR. Importantly, 806 CAR T cells are able to
312 more effectively control tumor growth in a wtEGFR/EGFRvIII model. 806 CAR T cells also
313 demonstrate greater killing in GBOs with heterogeneity of endogenous EGFR and EGFR mutants,
314 confirming its potential to more effectively treat GBM tumors by limiting the impact of tumor escape
315 due to antigen loss.

316

317 With regard to the CAR T trial in recurrent GBM (12), the demonstrated tumor recurrence was likely
318 due to the exclusive specificity of the scFv employed in the trial. The 2173 construct was chosen for
319 its selective binding to a novel glycine residue formed at the exons 2-7 deletion in EGFRvIII and for
320 a lack of cross-reactivity to wtEGFR (20). However, the binding affinity and target repertoire were of
321 secondary importance. Given the co-occurrence of amplified wtEGFR with EGFRvIII and most ECD
322 missense mutations (11), there is a clinically-relevant rationale for targeting multiple EGFR
323 alterations in the GBM population (25). Dual targeting of EGFR and EGFRvIII by CAR T and NK
324 cells has been demonstrated in recent studies using scFvs specific for both antigens (26-29). Our
325 work expands on that, as 806 CAR T cells were able to lyse GBM (U87MG, GSC5077) and non-
326 GBM (K562) cell lines modified to express not only wtEGFR and EGFRvIII, but also EGFR
327 extracellular mutations. In comparison, 2173 CAR T cells exhibited specificity for EGFRvIII alone
328 (12, 20).

329

330 GBM tumors are significantly heterogeneous, both intratumorally (30, 31) and intertumorsally (6).
331 Intratumorally, there are mixed cytological subtypes, exhibiting regional differences in gene

332 expression, key genetic mutations, and chromosomal alterations. This polyclonal nature contributes
333 to therapeutic resistance and tumor escape (32). To address intratumoral heterogeneity, relevant
334 targeted therapies would ideally be able to target larger tumor cell populations within the entire tumor
335 bulk. Given the co-occurrence of wtEGFR amplification seen with EGFR mutations and splice
336 variants (24), the cross-reactive EGFR-targeting 806 scFv should provide greater tumor cell
337 coverage, resulting in better tumor control. The potential for broader tumor control was demonstrated
338 through the high-fidelity, heterogeneous GBO model (22). While the VAFs associated with the
339 originating tumors of the GBOS allow for hypothesizing of independent EGFR mutant tumor
340 populations, one caveat is that the NGS methods used do not allow for concrete determination of
341 subpopulations. The data was subject to bias from tumor viability and number of reads of the sample.
342 Additionally, the heterogeneity of the EGFR variants on amplified alleles is complicated by the
343 mechanisms of amplification of EGFR. GBMs frequently harbor double minutes, extrachromosomal
344 sequences of DNA that are acentric and lead to asymmetric distribution to daughter cells (33). This
345 causes increased cell-to-cell heterogeneity of EGFR alterations in GBM.

346

347 Intertumoral variation, from patient to patient, reduces the applicable population for targeted
348 therapies. However, there are gene families frequently found altered across GBM (6). In particular,
349 EGFR amplification is found in up to 60% of GBMs. Concurrently with amplification, 30–40% of
350 GBM tumors express the constitutively active mutant variant, EGFRvIII (34). Combined with the
351 intratumoral expression of EGFR variants, these data suggest that targeting the EGFR family of
352 tumor-specific alterations may successfully address both inter- and intratumoral heterogeneity.

353

354 Several EGFRvIII targeted agents are currently in development or in clinical trials for the treatment
355 of GBM. Though the preclinical data from experimental studies evaluating these therapies have been
356 promising, their efficacy in the clinic has yet to be conclusively demonstrated (35–37). In a
357 vaccination approach to target the EGFRvIII in GBM patients, a phase III trial for newly diagnosed
358 glioblastoma failed to show overall efficacy despite 60–80% of recurrent tumors showing complete
359 loss of EGFRvIII positive cells (38). Additional trials targeting EGFRvIII demonstrated similar loss
360 of EGFRvIII concurrent with tumor recurrence (12, 39, 40). Similarly, the EGFRvIII-targeting CAR
361 T trial illustrated the continued presence of EGFR amplification and oncogenic EGFR ECD missense
362 mutations despite EGFRvIII antigen loss in post-treatment tumor specimens (12). These results
363 confirm the need to target multiple EGFR alterations simultaneously.

364

365 Despite preclinical efficacy, the success of wtEGFR targeting mAbs cetuximab and panitumumab
366 have been associated with on-target, off-tumor toxicity in other tumor types, due to their significant
367 binding to EGFR expressed on normal tissues (41, 42). Their clinical activity in GBM has yet to be
368 successfully demonstrated in large-scale studies. Co-culture of 806 CAR T cells with basal
369 physiologic EGFR-expressing normal tissue cell lines did not lead to significant cell killing in our
370 work. Previous work has suggested the 806 epitope is exposed on both mutated EGFR (EGFRvIII,
371 EGFR^{R108G/K}, EGFR^{A289D/T/V}) as well as amplified wtEGFR found on tumors, but not accessible on
372 wtEGFR found on normal tissue (43). The wtEGFR differences have been proposed to be due to
373 different post-translational mannose modifications and kinetics of EGFR trafficking in tumors
374 compared to normal tissue (44). Multiple clinical trials with humanized mAb 806 conjugated to a
375 microtubule inhibitor (ABT-414) have demonstrated only low levels of cutaneous toxicity (45–47).
376 The therapeutic window of CAR T cells for tumor-associated antigens relies on the quantitative
377 difference between antigen-overexpressing tumor and antigen-low normal tissue. Preclinical studies

806-CAR in Glioblastoma

378 targeting EGFR and erbB2 with affinity-lowered CAR T cells have demonstrated potent antitumor
379 effects against high antigen density while sparing low antigen density normal tissue (48-50). The
380 demonstrated cross-reactivity of 806 CAR T cells for EGFR alterations, including amplified
381 wtEGFR, EGFRvIII, and ECD missense mutations, suggests that 806 CAR T cells may be a more
382 efficacious therapeutic strategy to achieve tumor control and prevent tumor escape via target antigen
383 loss.
384

385 **Conflict of Interest**

386 The described work involves patent applications owned by the University of Pennsylvania. MM is an
387 inventor on multiple issued and pending patents related to CAR T cell technology used in this study.
388 These patents are assigned to the University of Pennsylvania and have been licensed to 3rd parties for
389 which royalties have or may be received.
390

391 **Author Contributions**

392 RT and ZB conceived and carried out the experiments, with contributions from LZ, JVZ, and DZ for
393 specific assays. MM, GM, HS, and DO supervised the project. RT and ZB wrote the manuscript and
394 all authors contributed to the final version of the manuscript.
395

396 **Funding**

397 The described work was funded by the GBM Translational Center of Excellence, the Templeton
398 Family Initiative in Neuro-Oncology, The Maria and Gabriele Troiano Brain Cancer Immunotherapy
399 Fund, and NIH (R35NS116843 to HS and R35NS097370 to GM).
400

401 **Acknowledgments**

402 The authors thank the Human Immunology Core at the University of Pennsylvania for providing
403 leukocytes for the described work, the Stem Cell and Xenograft Core at the University of
404 Pennsylvania for assistance with the animal work, and the Small Animal Imaging Facility at the
405 University of Pennsylvania for the bioluminescence imaging.
406

407 **Figure Legends**

408 **Figure 1.** Construction and expression of 806 CAR and EGFR mutant cell lines. (A) Schematic diagram of
409 vector map of 806 CAR containing the 4-1BB co-stimulatory domain. (B) CAR surface expression in primary
410 human CD4⁺ and CD8⁺ T cells. Human T cells were simulated for 24 hours with anti-CD3/anti-CD28 T-cell
411 activating beads and transduced with CAR transgenes and CAR expression was analyzed by flow cytometry
412 using biotinylated goat-anti-mouse (806, C225, and CD19 CARs) and goat-anti human F(ab)₂ fragment
413 specific antibodies (2173 CARs) followed by secondary staining with streptavidin-APC. (C) Schematic
414 showing targeted missense mutations in extracellular domain of EGFR, EGFR^{R108K/G}, EGFR^{A289D/T/V},

415 EGFR^{G598V} and splice variant EGFRvIII. (D) Schematic of lentiviral vector co-expressing CFP and wtEGFR
416 or EGFR mutant. (E) Flow based analysis of endogenous and ectopically expressed EGFR in U87MG,
417 GSC5077, and K562 cell lines using the cetuximab antibody. (F) U87MG, U87MG-EGFR and GSC5077-
418 EGFR expression of EGFRvIII. (G) U87MG-EGFR, GSC5077-EGFR, and K562 cell lines were transduced
419 with a lentiviral vector co-expressing CFP and indicated EGFR missense mutations and sorted by CFP
420 expression using fluorescent activated cell sorting.

421

422 **Figure 2.** *in vitro* characterization of 806 EGFR CAR T cells. Antigen specific cytolytic activity of
423 806 and 2173 CAR T cells against cell lines expressing EGFR and its variants. (A) U87MG-EGFR
424 and GSC5077-EGFR cell lines expressing EGFRvIII, EGFR^{R108K/G}, EGFR^{A289D/T/V}, and EGFR^{G598V}
425 mutant variants were stably transduced with Click Beetle Green (CBG) and co-cultured with CAR T
426 cells at indicated effector to target ratios for 24 hours. One representative experiment from 3 normal
427 donors is shown. Samples were performed in triplicates in 3 replicative experiments. C225-BB- ζ
428 CAR and CD19-BB- ζ CAR were used as positive and negative controls, respectively. (B) Antigen
429 specific cytolytic activity of 806 and 2173 CAR T cells in EGFR and its variants expressed in K562
430 cells in a 4-hour chromium release assay at indicated effector to target ratios. (C) K562 cells
431 expressing wtEGFR, EGFRvIII, or EGFR-mutants were co-cultured with 806 CART cells for 48
432 hours. IFN- γ , TNF- α , and IL2 secretion was measured in the supernatant by ELISA. Bar charts
433 represent results from single experiment and values represent the average \pm SD of triplicates. (D)
434 CD107a upregulation on CAR T cells stimulated with K562 cells expressing wtEGFR, EGFRvIII, or
435 EGFR-mutants for 4 hours. The percentage of CD107a expression was quantified on CD3 cells
436 (values represent the average of \pm SD of 2 repeated experiments).

437

438 **Figure 3.** Anti-tumor efficacy of 806 CAR T cells in primary astrocytes and keratinocytes. (A)
439 Surface expression of EGFR assessed by flow cytometry on human primary astrocytes and
440 keratinocytes using EGFR-specific cetuximab antibody. (B) Primary astrocytes and keratinocytes
441 were co-cultured with 806 CAR T cells at indicated ratios in a 4-hour chromium assay and results are
442 representative of a single experiment showing the average \pm SD of triplicates. (C) Levels of IFN- γ
443 measured in supernatants by ELISA 24 hours after co-culturing 806 and 2173 CAR T cells with
444 primary astrocytes and keratinocytes at effector to target ratio of 1:1. Results are representative of a
445 single experiment with the average \pm SD of triplicates. (D) EGFR expression analysis by quantitative
446 flow cytometry, with quantified EGFR counts on each bar graph.

447

448 **Figure 4.** *In vivo* anti-tumor effect of 806 CAR T cells in NSG mice bearing U87MG-
449 EGFR/EGFRvIII⁺ xenografts. Seven days after 250,000 U87MG-EGFR/EGFRvIII cells were
450 subcutaneously implanted into mice, 3×10^6 T cells were injected intravenously with indicated CAR
451 constructs. (A) Survival based on time to endpoint was plotted using a Kaplan-Meier curve and
452 statistically significant differences between CAR groups were determined using log-rank Mantel-Cox
453 test. Tumor burden was assessed by bioluminescent imaging. Bars indicate means \pm SD (n = 7 mice
454 per group). Tumor burden was quantified as total flux (B) and in individual mice (C) in units of
455 photons/second. Bars indicate means \pm SD (n = 7 mice). P = photons.

456

457 **Figure 5.** 806 CAR T activity in heterogenous GBOs highlights cross-reactivity of 806 binder
458 against oncogenic EGFRs. CAR T co-culture with GBOs was used to demonstrate anti-EGFR
459 activity. (A) EGFR alterations identified in each GBO line. (B) Immunofluorescence images of CAR

806-CAR in Glioblastoma

460 T cells engrafted GBOs, for 4 organoids per condition, 9057 (left) and 9066 (right). Blue=DAPI;
461 Red=CD3⁺; White=Cleaved caspase 3⁺ (CC3⁺), scale bar = 100 μ m. (C) Quantification of CD3⁺ cells
462 (left) and CC3⁺ cells (right) showing anti-tumor activity from the 806 CAR T cells. (D)
463 Immunofluorescence images of CAR T cell targets in GBOs, for 9057 (left) and 9066 (right).
464 Blue=DAPI; Red=EGFR⁺; White=EGFRvIII⁺, scale bar = 100 μ m. (E) Quantification of EGFR⁺
465 (left) and EGFRvIII⁺ signals (right) showing anti-tumor activity from the 806 CAR T cells. Error
466 bars are \pm standard error.

467

468

References

469

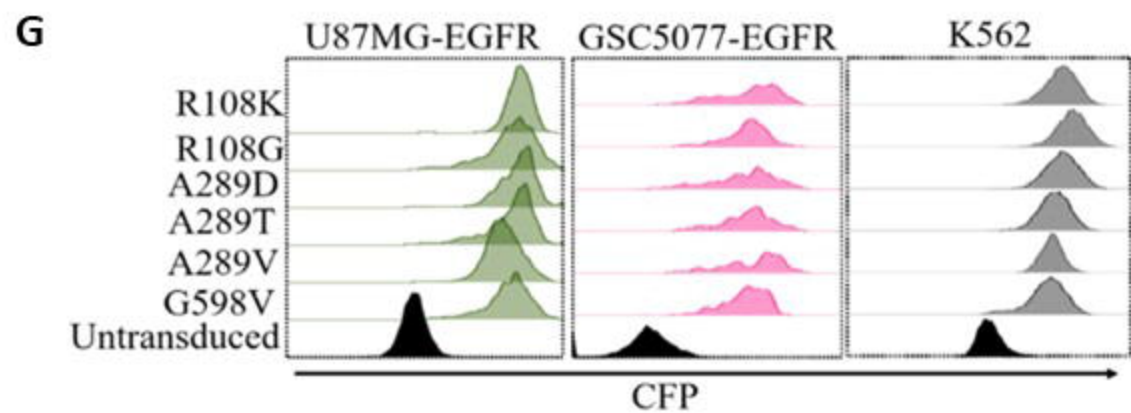
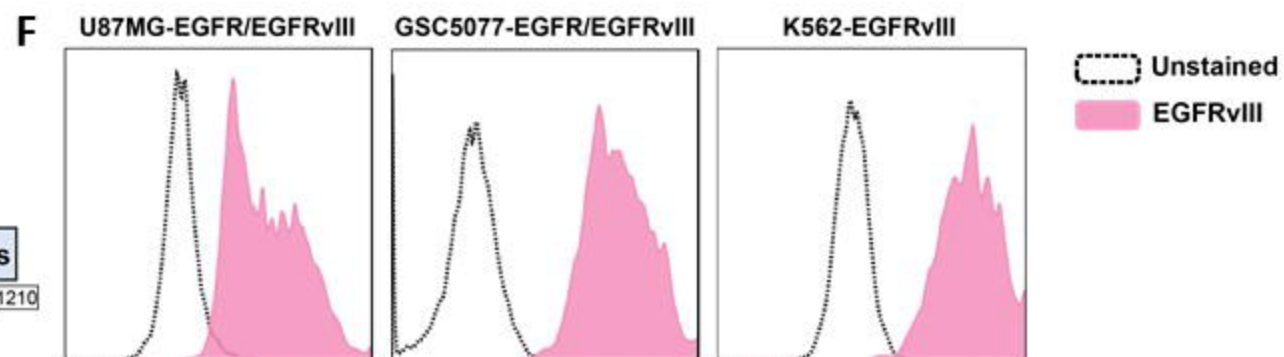
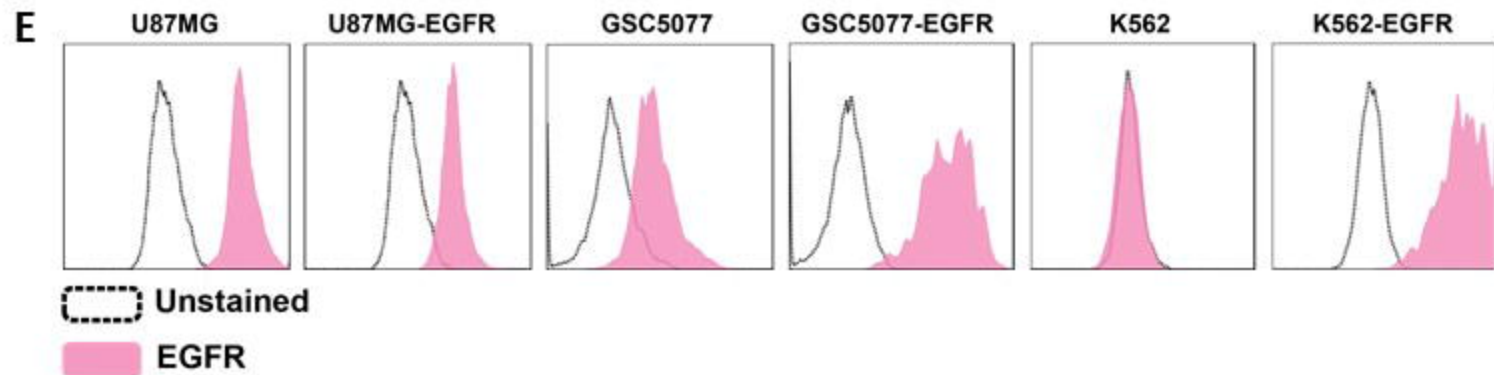
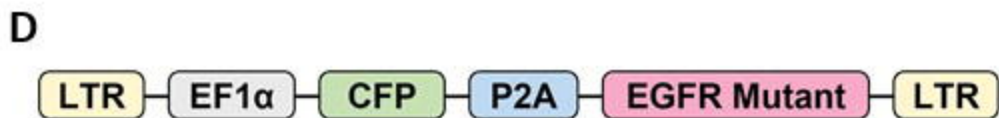
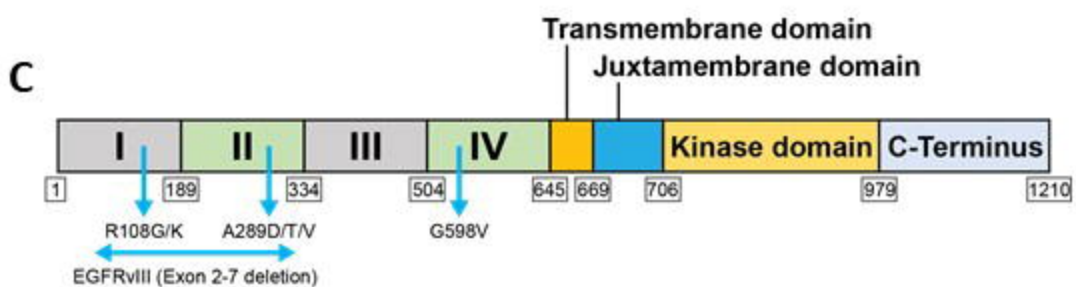
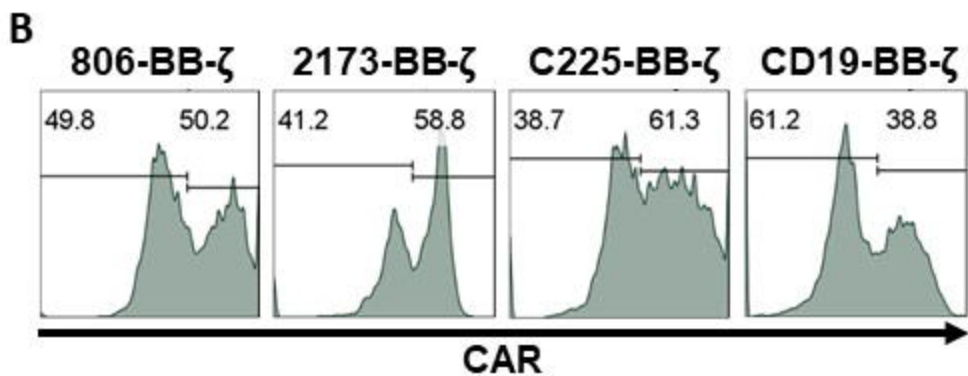
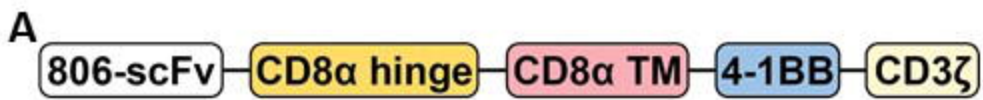
- 470 1. Castellarin M, Watanabe K, June CH, Kloss CC, Posey AD, Jr. Driving cars to the clinic for
471 solid tumors. *Gene Ther.* 2018;25(3):165-75.
- 472 2. Fesnak AD, June CH, Levine BL. Engineered T cells: the promise and challenges of cancer
473 immunotherapy. *Nat Rev Cancer.* 2016;16(9):566-81.
- 474 3. Porter DL, Levine BL, Kalos M, Bagg A, June CH. Chimeric antigen receptor-modified T
475 cells in chronic lymphoid leukemia. *N Engl J Med.* 2011;365(8):725-33.
- 476 4. Jackson C, Ruzevick J, Phallen J, Belcaid Z, Lim M. Challenges in immunotherapy presented
477 by the glioblastoma multiforme microenvironment. *Clin Dev Immunol.* 2011;2011:732413.
- 478 5. Nduom EK, Weller M, Heimberger AB. Immunosuppressive mechanisms in glioblastoma.
479 *Neuro Oncol.* 2015;17 Suppl 7:vii9-vii14.
- 480 6. Brennan CW, Verhaak RG, McKenna A, Campos B, Nounshmehr H, Salama SR, et al. The
481 somatic genomic landscape of glioblastoma. *Cell.* 2013;155(2):462-77.
- 482 7. Cominelli M, Grisanti S, Mazzoleni S, Branca C, Buttolo L, Furlan D, et al. EGFR amplified
483 and overexpressing glioblastomas and association with better response to adjuvant metronomic
484 temozolomide. *J Natl Cancer Inst.* 2015;107(5).
- 485 8. Lopez-Gines C, Gil-Benso R, Ferrer-Luna R, Benito R, Serna E, Gonzalez-Darder J, et al.
486 New pattern of EGFR amplification in glioblastoma and the relationship of gene copy number with
487 gene expression profile. *Mod Pathol.* 2010;23(6):856-65.
- 488 9. Nishikawa R, Ji XD, Harmon RC, Lazar CS, Gill GN, Cavenee WK, et al. A mutant
489 epidermal growth factor receptor common in human glioma confers enhanced tumorigenicity. *Proc*
490 *Natl Acad Sci U S A.* 1994;91(16):7727-31.
- 491 10. Lee JC, Vivanco I, Beroukhir R, Huang JH, Feng WL, DeBiasi RM, et al. Epidermal growth
492 factor receptor activation in glioblastoma through novel missense mutations in the extracellular
493 domain. *PLoS Med.* 2006;3(12):e485.
- 494 11. Binder ZA, Thorne AH, Bakas S, Wileyto EP, Bilello M, Akbari H, et al. Epidermal Growth
495 Factor Receptor Extracellular Domain Mutations in Glioblastoma Present Opportunities for Clinical
496 Imaging and Therapeutic Development. *Cancer Cell.* 2018;34(1):163-77 e7.
- 497 12. O'Rourke DM, Nasrallah MP, Desai A, Melenhorst JJ, Mansfield K, Morrisette JJD, et al. A
498 single dose of peripherally infused EGFRvIII-directed CAR T cells mediates antigen loss and
499 induces adaptive resistance in patients with recurrent glioblastoma. *Sci Transl Med.* 2017;9(399).

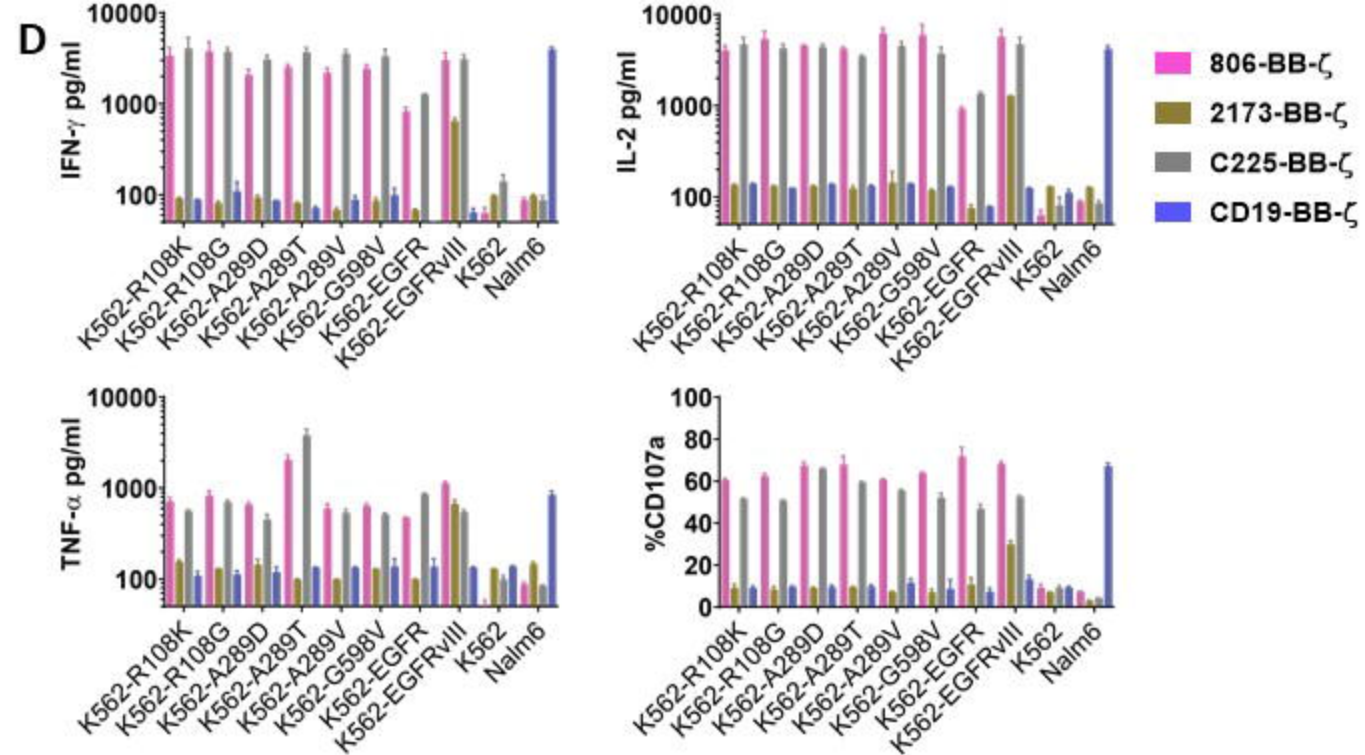
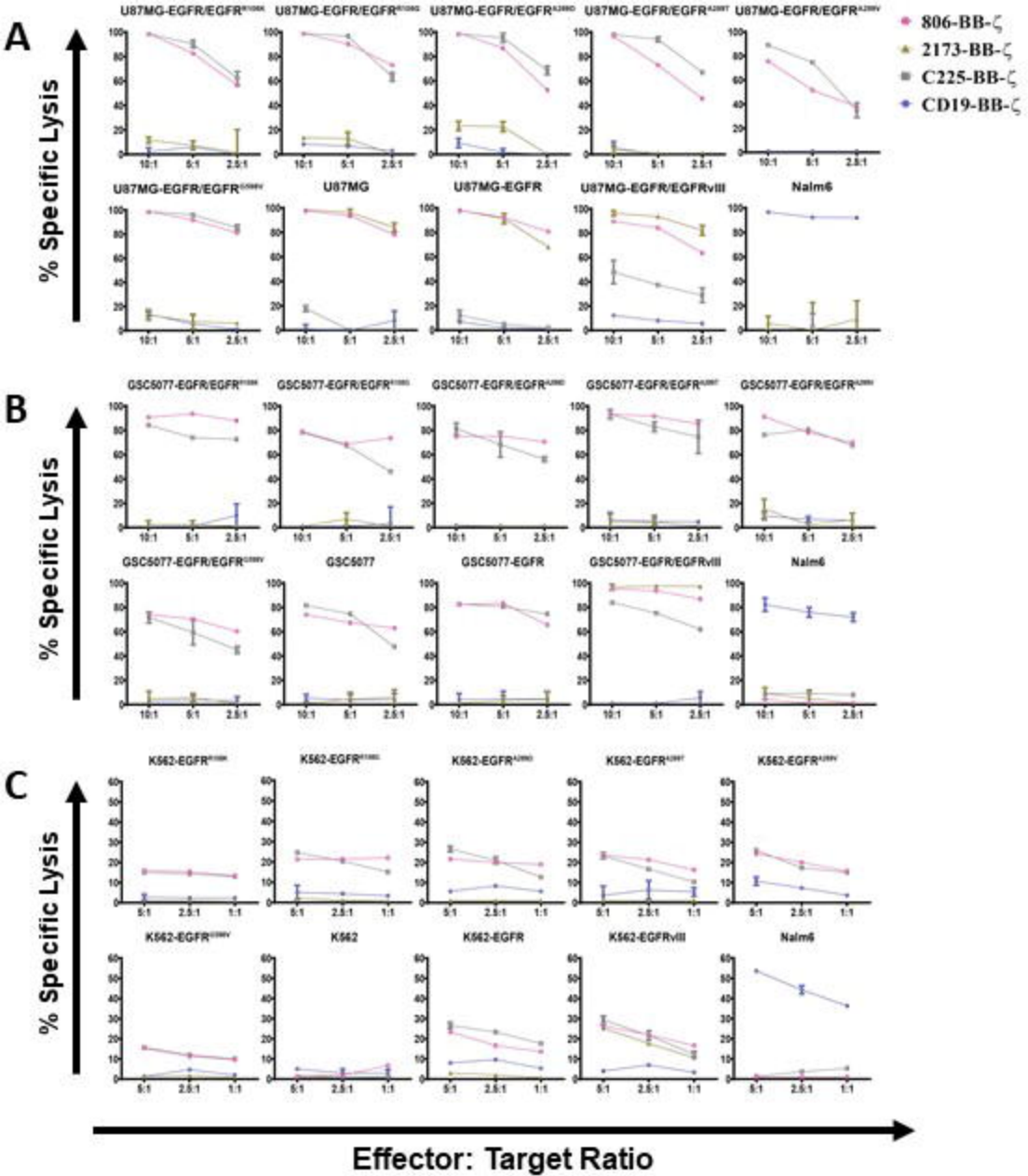
- 500 13. Gan HK, Burgess AW, Clayton AH, Scott AM. Targeting of a conformationally exposed,
501 tumor-specific epitope of EGFR as a strategy for cancer therapy. *Cancer Res.* 2012;72(12):2924-30.
- 502 14. Panousis C, Rayzman VM, Johns TG, Renner C, Liu Z, Cartwright G, et al. Engineering and
503 characterisation of chimeric monoclonal antibody 806 (ch806) for targeted immunotherapy of
504 tumours expressing de2-7 EGFR or amplified EGFR. *Br J Cancer.* 2005;92(6):1069-77.
- 505 15. Phillips AC, Boghaert ER, Vaidya KS, Mitten MJ, Norvell S, Falls HD, et al. ABT-414, an
506 Antibody-Drug Conjugate Targeting a Tumor-Selective EGFR Epitope. *Mol Cancer Ther.*
507 2016;15(4):661-9.
- 508 16. Lassman A, Pugh S, Wang T, Aldape K, Gan H, Preusser M, et al. ACTR-21. A
509 RANDOMIZED, DOUBLE-BLIND, PLACEBO-CONTROLLED PHASE 3 TRIAL OF
510 DEPATUXIZUMAB MAFODOTIN (ABT-414) IN EPIDERMAL GROWTH FACTOR
511 RECEPTOR (EGFR) AMPLIFIED (AMP) NEWLY DIAGNOSED GLIOBLASTOMA (nGBM).
512 *Neuro-Oncology.* 2019;21(Supplement_6):vi17-vi.
- 513 17. Milone MC, Fish JD, Carpenito C, Carroll RG, Binder GK, Teachey D, et al. Chimeric
514 receptors containing CD137 signal transduction domains mediate enhanced survival of T cells and
515 increased antileukemic efficacy in vivo. *Mol Ther.* 2009;17(8):1453-64.
- 516 18. Imai C, Mihara K, Andreansky M, Nicholson IC, Pui CH, Geiger TL, et al. Chimeric
517 receptors with 4-1BB signaling capacity provoke potent cytotoxicity against acute lymphoblastic
518 leukemia. *Leukemia.* 2004;18(4):676-84.
- 519 19. Carpenito C, Milone MC, Hassan R, Simonet JC, Lakhai M, Suhoski MM, et al. Control of
520 large, established tumor xenografts with genetically retargeted human T cells containing CD28 and
521 CD137 domains. *Proc Natl Acad Sci U S A.* 2009;106(9):3360-5.
- 522 20. Johnson LA, Scholler J, Ohkuri T, Kosaka A, Patel PR, McGettigan SE, et al. Rational
523 development and characterization of humanized anti-EGFR variant III chimeric antigen receptor T
524 cells for glioblastoma. *Sci Transl Med.* 2015;7(275):275ra22.
- 525 21. Yin Y, Boesteanu AC, Binder ZA, Xu C, Reid RA, Rodriguez JL, et al. Checkpoint Blockade
526 Reverses Anergy in IL-13Ralpha2 Humanized scFv-Based CAR T Cells to Treat Murine and Canine
527 Gliomas. *Mol Ther Oncolytics.* 2018;11:20-38.
- 528 22. Jacob F, Salinas RD, Zhang DY, Nguyen PTT, Schnoll JG, Wong SZH, et al. A Patient-
529 Derived Glioblastoma Organoid Model and Biobank Recapitulates Inter- and Intra-tumoral
530 Heterogeneity. *Cell.* 2020;180(1):188-204 e22.
- 531 23. Jacob F, Ming GL, Song H. Generation and biobanking of patient-derived glioblastoma
532 organoids and their application in CAR T cell testing. *Nat Protoc.* 2020;15(12):4000-33.
- 533 24. Nasrallah MP, Binder ZA, Oldridge DA, Zhao J, Lieberman DB, Roth JJ, et al. Molecular
534 Neuropathology in Practice: Clinical Profiling and Integrative Analysis of Molecular Alterations in
535 Glioblastoma. *Acad Pathol.* 2019;6:2374289519848353.
- 536 25. Reilly EB, Phillips AC, Buchanan FG, Kingsbury G, Zhang Y, Meulbroek JA, et al.
537 Characterization of ABT-806, a Humanized Tumor-Specific Anti-EGFR Monoclonal Antibody. *Mol
538 Cancer Ther.* 2015;14(5):1141-51.
- 539 26. Genssler S, Burger MC, Zhang C, Oelsner S, Mildenerger I, Wagner M, et al. Dual targeting
540 of glioblastoma with chimeric antigen receptor-engineered natural killer cells overcomes
541 heterogeneity of target antigen expression and enhances antitumor activity and survival.
542 *Oncoimmunology.* 2016;5(4):e1119354.

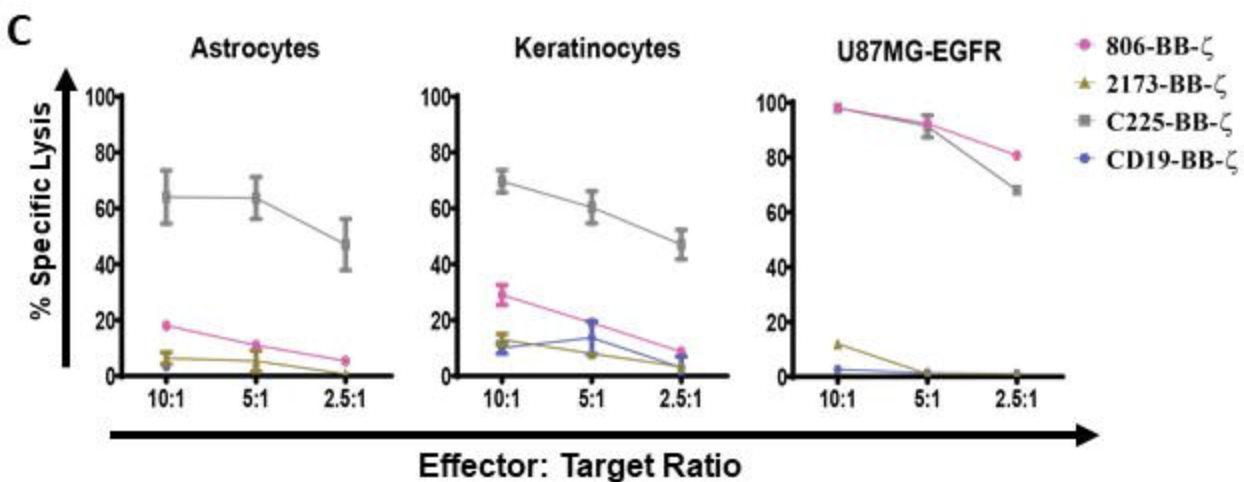
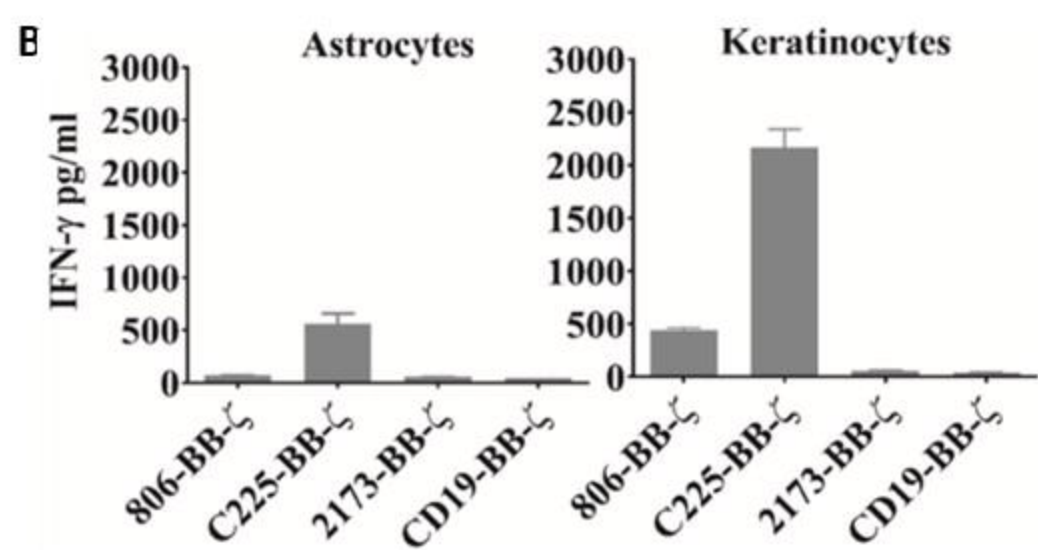
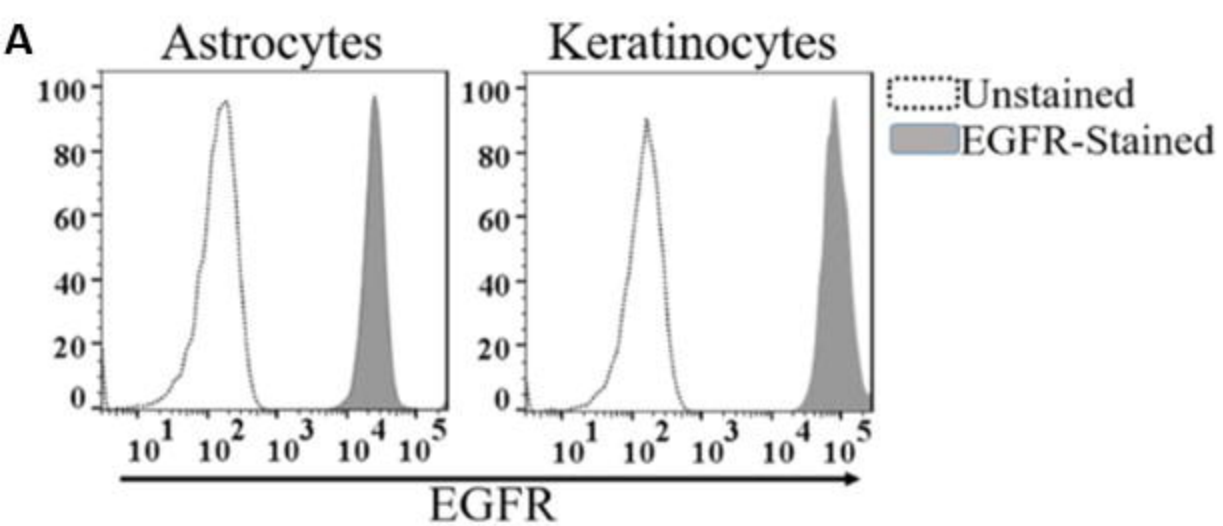
806-CAR in Glioblastoma

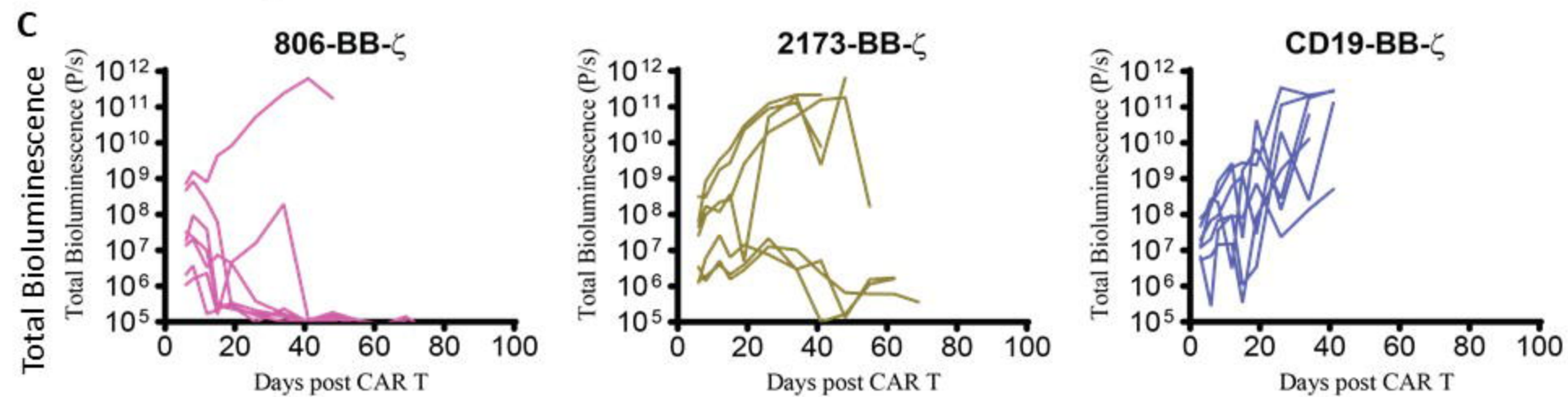
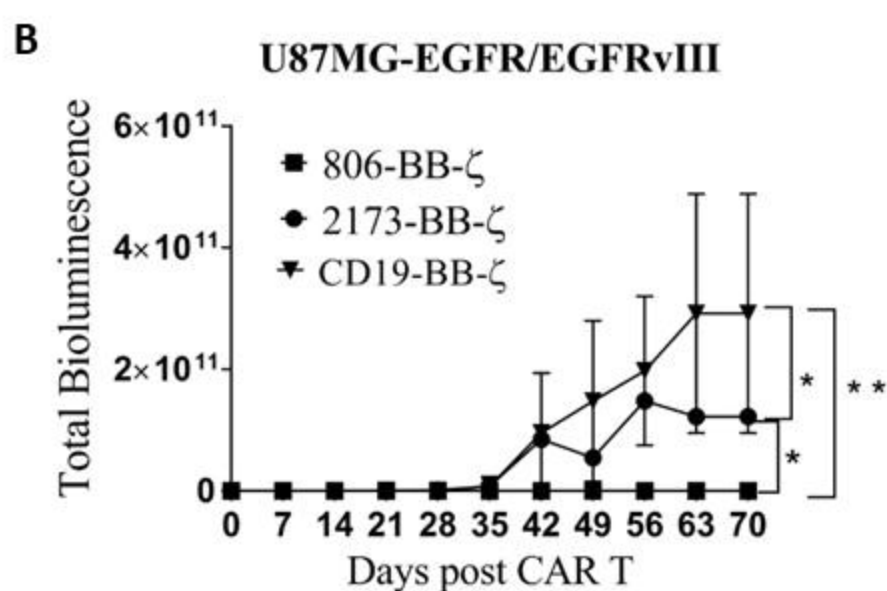
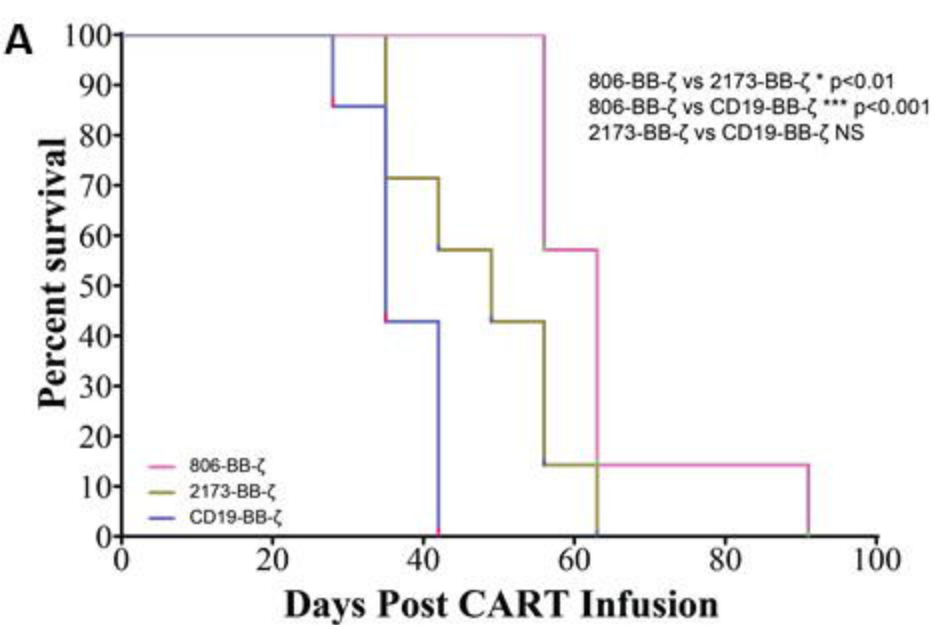
- 543 27. Han J, Chu J, Keung Chan W, Zhang J, Wang Y, Cohen JB, et al. CAR-Engineered NK Cells
544 Targeting Wild-Type EGFR and EGFRvIII Enhance Killing of Glioblastoma and Patient-Derived
545 Glioblastoma Stem Cells. *Sci Rep.* 2015;5:11483.
- 546 28. Jiang H, Gao H, Kong J, Song B, Wang P, Shi B, et al. Selective Targeting of Glioblastoma
547 with EGFRvIII/EGFR Bitargeted Chimeric Antigen Receptor T Cell. *Cancer Immunol Res.*
548 2018;6(11):1314-26.
- 549 29. Ravanpay AC, Gust J, Johnson AJ, Rolczynski LS, Cecchini M, Chang CA, et al. EGFR806-
550 CAR T cells selectively target a tumor-restricted EGFR epitope in glioblastoma. *Oncotarget.*
551 2019;10(66):7080-95.
- 552 30. Darmanis S, Sloan SA, Croote D, Mignardi M, Chernikova S, Samghababi P, et al. Single-
553 Cell RNA-Seq Analysis of Infiltrating Neoplastic Cells at the Migrating Front of Human
554 Glioblastoma. *Cell Rep.* 2017;21(5):1399-410.
- 555 31. Patel AP, Tirosh I, Trombetta JJ, Shalek AK, Gillespie SM, Wakimoto H, et al. Single-cell
556 RNA-seq highlights intratumoral heterogeneity in primary glioblastoma. *Science.*
557 2014;344(6190):1396-401.
- 558 32. Skaga E, Kuleskiy E, Fayzullin A, Sandberg CJ, Potdar S, Kytölä A, et al. Intertumoral
559 heterogeneity in patient-specific drug sensitivities in treatment-naïve glioblastoma. *BMC Cancer.*
560 2019;19(1):628.
- 561 33. Bailey C, Shoura MJ, Mischel PS, Swanton C. Extrachromosomal DNA-relieving heredity
562 constraints, accelerating tumour evolution. *Ann Oncol.* 2020;31(7):884-93.
- 563 34. Gan HK, Kaye AH, Luwor RB. The EGFRvIII variant in glioblastoma multiforme. *J Clin*
564 *Neurosci.* 2009;16(6):748-54.
- 565 35. Choi BD, Archer GE, Mitchell DA, Heimberger AB, McLendon RE, Bigner DD, et al.
566 EGFRvIII-targeted vaccination therapy of malignant glioma. *Brain Pathol.* 2009;19(4):713-23.
- 567 36. Karpel-Massler G, Schmidt U, Unterberg A, Halatsch ME. Therapeutic inhibition of the
568 epidermal growth factor receptor in high-grade gliomas: where do we stand? *Mol Cancer Res.*
569 2009;7(7):1000-12.
- 570 37. Rosenthal M, Curry R, Reardon DA, Rasmussen E, Upreti VV, Damore MA, et al. Safety,
571 tolerability, and pharmacokinetics of anti-EGFRvIII antibody-drug conjugate AMG 595 in patients
572 with recurrent malignant glioma expressing EGFRvIII. *Cancer Chemother Pharmacol.*
573 2019;84(2):327-36.
- 574 38. Heimberger AB, Sampson JH. The PEPvIII-KLH (CDX-110) vaccine in glioblastoma
575 multiforme patients. *Expert Opin Biol Ther.* 2009;9(8):1087-98.
- 576 39. Weller M, Butowski N, Tran DD, Recht LD, Lim M, Hirte H, et al. Rindopepimut with
577 temozolomide for patients with newly diagnosed, EGFRvIII-expressing glioblastoma (ACT IV): a
578 randomised, double-blind, international phase 3 trial. *Lancet Oncol.* 2017;18(10):1373-85.
- 579 40. Schuster J, Lai RK, Recht LD, Reardon DA, Paleologos NA, Groves MD, et al. A phase II,
580 multicenter trial of rindopepimut (CDX-110) in newly diagnosed glioblastoma: the ACT III study.
581 *Neuro Oncol.* 2015;17(6):854-61.
- 582 41. Saltz LB, Meropol NJ, Loehrer PJ, Sr., Needle MN, Kopit J, Mayer RJ. Phase II trial of
583 cetuximab in patients with refractory colorectal cancer that expresses the epidermal growth factor
584 receptor. *J Clin Oncol.* 2004;22(7):1201-8.

- 585 42. Holch JW, Held S, Stintzing S, Fischer von Weikersthal L, Decker T, Kiani A, et al. Relation
586 of cetuximab-induced skin toxicity and early tumor shrinkage in metastatic colorectal cancer patients:
587 results of the randomized phase 3 trial FIRE-3 (AIO KKR0306). *Ann Oncol.* 2020;31(1):72-8.
- 588 43. Orellana L, Thorne AH, Lema R, Gustavsson J, Parisian AD, Hospital A, et al. Oncogenic
589 mutations at the EGFR ectodomain structurally converge to remove a steric hindrance on a kinase-
590 coupled cryptic epitope. *Proc Natl Acad Sci U S A.* 2019;116(20):10009-18.
- 591 44. Johns TG, Mellman I, Cartwright GA, Ritter G, Old LJ, Burgess AW, et al. The antitumor
592 monoclonal antibody 806 recognizes a high-mannose form of the EGF receptor that reaches the cell
593 surface when cells over-express the receptor. *FASEB J.* 2005;19(7):780-2.
- 594 45. Cleary JM, Reardon DA, Azad N, Gandhi L, Shapiro GI, Chaves J, et al. A phase 1 study of
595 ABT-806 in subjects with advanced solid tumors. *Invest New Drugs.* 2015;33(3):671-8.
- 596 46. Reardon DA, Lassman AB, van den Bent M, Kumthekar P, Merrell R, Scott AM, et al.
597 Efficacy and safety results of ABT-414 in combination with radiation and temozolomide in newly
598 diagnosed glioblastoma. *Neuro Oncol.* 2017;19(7):965-75.
- 599 47. van den Bent M, Gan HK, Lassman AB, Kumthekar P, Merrell R, Butowski N, et al. Efficacy
600 of depatuxizumab mafodotin (ABT-414) monotherapy in patients with EGFR-amplified, recurrent
601 glioblastoma: results from a multi-center, international study. *Cancer Chemother Pharmacol.*
602 2017;80(6):1209-17.
- 603 48. Caruso HG, Hurton LV, Najjar A, Rushworth D, Ang S, Olivares S, et al. Tuning Sensitivity
604 of CAR to EGFR Density Limits Recognition of Normal Tissue While Maintaining Potent Antitumor
605 Activity. *Cancer Res.* 2015;75(17):3505-18.
- 606 49. Liu X, Jiang S, Fang C, Yang S, Olalere D, Pequignot EC, et al. Affinity-Tuned ErbB2 or
607 EGFR Chimeric Antigen Receptor T Cells Exhibit an Increased Therapeutic Index against Tumors in
608 Mice. *Cancer Res.* 2015;75(17):3596-607.
- 609 50. Richman SA, Milone MC. Neurotoxicity Associated with a High-Affinity GD2 CAR-
610 Response. *Cancer Immunol Res.* 2018;6(4):496-7.
- 611









A GBO 9057
 EGFR copy number gain
 EGFRvIII
 EGFR G598V
 EGFR C595Y

GBO 9066
 EGFR copy number gain
 EGFR A289V
 EGFR G598V

